

INTENSITY MEASUREMENTS IN MICROWAVE SPECTROSCOPY THE "ANTIMODULATION" METHOD

by A. DYMANUS

Fysisch Laboratorium der Rijksuniversiteit, Utrecht, Nederland.

Synopsis

Principle and theoretical background are presented of a new method for the precision measurement of absolute and relative peak intensities of microwave absorption lines. This method, called the "antimodulation" method, can be used with any spectrometer employing molecular modulation. In the present research the antimodulation method has been applied in the 1.25 cm wavelength region with a Stark-cavity spectrometer of novel design. As a check on the possibilities of the antimodulation method measurements have been performed on seven lines arising from the $J = 1 \rightarrow 2$ rotational transition in carbonyl sulphide (OCS). But for the l -doublet lines, results of both absolute (standard error ~ 2.5 percent) and relative (error 1-2 percent) measurements are in good agreement with calculated values. The measured intensities of the l -doublet lines are about 15 percent too low. This discrepancy cannot be explained by experimental errors. A possible refinement of the theory is suggested to explain the difference.

§ 1. *Introduction.* In the early years (1946-1949) of microwave spectroscopy several methods were introduced for the measurement of line intensities of strongly absorbing substances (NH_3 , O_2 , H_2O , etc.)¹⁾²⁾. The accuracy of these methods varied from 2 to 5 percent both for relative and absolute measurements.

In the following years some attempts³⁾⁴⁾ were also made to develop methods for the measurement of weak absorption lines. At present relative intensities of weak neighbouring lines can be determined with an accuracy of at best 15 percent with the widely used Stark-waveguide spectrometer⁴⁾. The accuracy of absolute measurements is usually not better than about 25 percent. Recently, new approaches to the problem of intensity measurements were reported by Verdier and Wilson Jr., and by Mattauch and Strandberg⁵⁾. The accuracy obtained by the latter authors is, however, not better than that indicated above. The approach of Verdier and Wilson Jr. looks successful, but only for relative measurements on neighbouring medium strong and not easily saturable lines.

In this paper a general outline is given of a new method (the "anti-

modulation" method) for the precision measurement of peak intensities of sharp absorption lines in the centimetre wavelength region. A detailed account of the method can be found elsewhere ⁶⁾. As a check on the possibilities of the antimodulation method both relative and absolute measurements have been performed on a series of lines arising from the $J = 1 \rightarrow 2$ rotational transition in carbonyl sulphide (OCS). Errors in absolute measurements amounted to 2.5 percent while those in relative measurements could be reduced to 1–2 percent.

PART I. THE METHOD

§ 2. *Principle of the antimodulation method.* The antimodulation (abbr. *AiM*-) method can be applied with any spectrometer employing molecular (Stark or Zeeman) modulation. In the present research this method has been applied with a Stark-cavity spectrometer (Fig. 1a) in order to eliminate difficulties due to standing waves ⁴⁾. The operation of the *AiM*-method proceeds as follows.

The microwave power leaving the Stark cavity absorption cell is amplitude modulated at the rate of the modulating Stark field. When both klystron and cavity are tuned to the resonance frequency of the gas, the modulation depth m_g due to the Stark modulation is determined a.o. by Q_L , the loaded Q -factor of the empty cavity, and by α_{\max} , the peak intensity of the line. The time variation of this power for the case of a square wave Stark modulation is shown in Fig. 1b, in which the zero-power level is left out.

The main idea of the *AiM*-method is the cancellation of the Stark modulation of the transmitted power by a second modulation at the same frequency but 180° out-of-phase. This second modulation, called "antimodulation", is provided by an "antimodulator" placed behind the absorption cell. The microwave power modulated by a square wave *AiM* is shown in Fig. 1c. Let m_{AiM} be the modulation depth of the *AiM*. When $m_{AiM} = m_g$, the antimodulation cancels the Stark modulation and the output of the power detector contains no components at the modulation frequency (Fig. 1d). If $m_{AiM}(= m_g)$ is known accurately, the desired α_{\max} is obtained from a relation between m_g , α_{\max} , and Q_L (also known) of the Stark cavity.

The *AiM*-method possesses distinct advantages over other methods. The response law ⁴⁾ of the power detector need not to be known neither for relative nor for absolute intensities. Use of the zero-balance principle increases greatly the accuracy and makes the results insensitive to variations of the microwave input power and of the overall gain of the spectrometer. In the absence of power saturation a variation of the input power by a factor of 20 has no influence on the measured line intensities. The accuracy of the method is determined primarily by the calibration error of the antimodulator and by the error in Q_L .

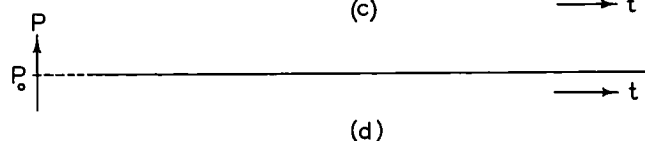
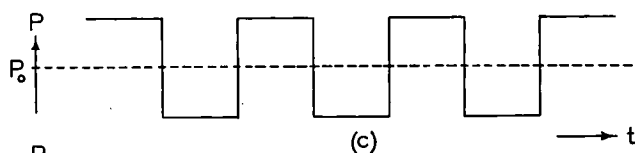
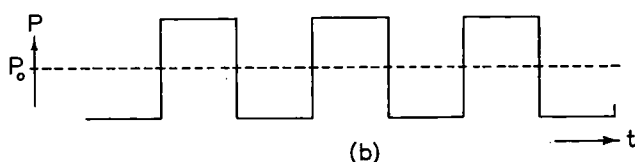
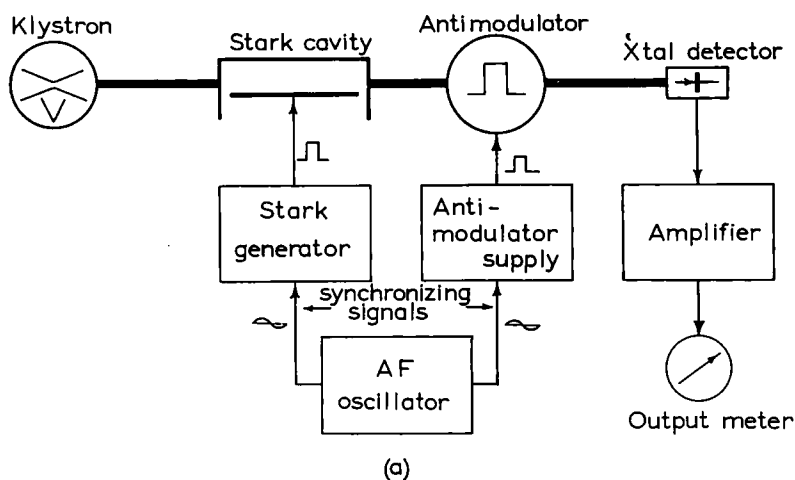


Fig. 1. (a) Simplified diagram of a Stark-cavity spectrometer with antimodulation; (b), (c) time variation of the power P at the detector due to the Stark modulation and to the antimodulation, respectively; (d) time variation of the power P when $m_{AiM} = m_g$.

§ 3. The relation between m_g , α_{\max} , and Q_L . The power transmission properties of a gas filled cavity, connected on the input side to a matched generator and on the output side to a (matched or mismatched) detector, can be derived from the relation (Ref. 6, p. 50):

$$P_A = A \left[\frac{1}{Q_L^2} + \left(\frac{\nu}{\nu_{ae}} - \frac{\nu_{ae}}{\nu} \right)^2 \right]^{-1}, \quad (1)$$

where,

$$A = \eta P_0 \frac{4G_L}{Q_{\text{ext},1} \cdot Q_{\text{ext},2}},$$

and:

P_A = power absorbed by the detector;

P_0 = input power;

η = power transmission efficiency of the output guide;

G_L = detector admittance referred to the output terminals of the cavity;

$Q_{\text{ext}, 1}, Q_{\text{ext}, 2}$ = external Q -factor of the cavity coupling to input and output guide, respectively;

ν = applied frequency;

ν_{ae} = resonance frequency of the a -th mode of the empty cavity.

Admission of gas into a cavity changes the resonance frequency and increases the power loss. The latter can be described by introducing into Q_L a new term Q_g in the following way:

$$\frac{1}{Q_{Lg}} = \frac{1}{Q_L} + \frac{1}{Q_g}, \quad (2)$$

where, Q_{Lg} is the Q_L -factor of a gas filled cavity. The quantity Q_g , also called "Q-factor of the gas" is related to the absorption coefficient α of the gas by the relation 7):

$$\frac{1}{Q_g} = \frac{\lambda}{\sqrt{\epsilon_1}} \alpha(\nu),$$

$$\lambda = \lambda/(2\pi),$$

in which, λ is the free-space wavelength of the incident radiation, and ϵ_1 the real part of the complex dielectric constant of the gas: $\epsilon = \epsilon_1 - i\epsilon_2$. For gases at low pressures $\epsilon_1 - 1$ is of the order of $10^{-4} - 10^{-6}$ in the microwave region. Thus, at low pressures $1/Q_g$ is:

$$\frac{1}{Q_g} = \lambda\alpha. \quad (3)$$

The resonance frequency ν_{ag} of a gas filled cavity is given by (Ref. 8, p. 308):

$$\nu_{ag} = \nu_{ae}/\sqrt{\epsilon_1}. \quad (4)$$

From the expression of Karplus and Schwinger⁹⁾ for the electric susceptibility χ_e of a gas in the neighbourhood of a particular resonance frequency ν_0 :

$$\chi_e = C \left\{ \left[2 - \frac{\nu(\nu - \nu_0)}{(\nu - \nu_0)^2 + (\Delta\nu)^2} + \frac{\nu(\nu + \nu_0)}{(\nu + \nu_0)^2 + (\Delta\nu)^2} \right] + \right. \\ \left. + i\nu \left[\frac{\Delta\nu}{(\nu - \nu_0)^2 + (\Delta\nu)^2} + \frac{\Delta\nu}{(\nu + \nu_0)^2 + (\Delta\nu)^2} \right] \right\}, \quad (5)$$

and from the well-known relations (Ref. 10, p. 340):

$$\begin{aligned}\varepsilon_1 &= 1 + 4\pi N \operatorname{Re} \chi_e, \\ \alpha &= \frac{4\pi}{\lambda_0} N \operatorname{Im} \chi_e,\end{aligned}\quad (6)$$

it can readily be proved that for a gas at low pressure ($\Delta\nu \ll \nu_0$) ε_1 can be written as:

$$\varepsilon_1 = \varepsilon_0 - \lambda_0 \beta(\nu). \quad (7)$$

In Eqs. (5)–(7), C is a constant, $\Delta\nu$ the half width of the absorption line at half of its maximum intensity, in the following referred to as: half-width; N the number of molecules per cm^3 , λ_0 ($= 2\pi\lambda_0$) the resonant wavelength of the gas, ε_0 the dielectric constant for $|\nu - \nu_0| \gg \Delta\nu$, and $\beta(\nu)$ the dispersion component of ε_1 given by:

$$\beta(\nu) = \alpha_{\max} \frac{(\nu - \nu_0)\Delta\nu}{(\nu - \nu_0)^2 + (\Delta\nu)^2}. \quad (8)$$

For high- Q cavities only ν close to ν_{ag} is of importance, and for gases at low pressures $\varepsilon_0 \simeq 1$. By substituting Eq. (7) into Eq. (4), and by replacing Q_L and ν_{ae} in Eq. (1) by Q_{Lg} and ν_{ag} respectively, the power P_{Ag} absorbed by the detector connected to a gas-filled cavity becomes:

$$P_{Ag} = A \left\{ \left[\frac{1}{Q_L} + \lambda_0 \alpha(\nu) \right]^2 + \left[\frac{\nu}{\nu_{ae_0}} - \frac{\nu_{ae_0}}{\nu} - \lambda_0 \beta(\nu) \right]^2 \right\}^{-1}, \quad (9)$$

with:

$$\alpha(\nu) = \alpha_{\max} \frac{(\Delta\nu)^2}{(\nu - \nu_0)^2 + (\Delta\nu)^2}. \quad (10)$$

The quantity ν_{ae_0} in Eq. (9) is the resonance frequency of the cavity if $\beta(\nu)$ is neglected. In the following ν_{ae_0} will be denoted by ν_a , the usual symbol for the resonance frequency of the a -th mode of the cavity.

When the gas is subjected to the action of a uniform electric field the spatial (M) degeneracy is removed and the line is split in a number of components. The total absorption intensity $F_s(\nu)$ by these components at any frequency is simply the sum of absorption intensities $\alpha_M(\nu)$ of the individual components:

$$F_s(\nu) = \sum_M \alpha_M(\nu), \quad (11)$$

with,

$$\alpha_M(\nu) = (\alpha_M)_{\max} \frac{(\Delta\nu)_M^2}{(\nu - \nu_M)^2 + (\Delta\nu)_M^2}. \quad (11a)$$

Herein, $(\alpha_M)_{\max}$ is the peak value of the absorption coefficient $\alpha_M(\nu)$, ν_M the centre frequency, and $(\Delta\nu)_M$ the half-width of the M -th Stark component.

The sum in Eq. (11) is taken over all Stark components. In the following $F_s(\nu)$ is called Stark "absorption function".

A function $D_s(\nu)$ will now be introduced which describes the dispersion component of ϵ_1 in the vicinity of a particular line split by the Stark effect. This function, in the following called the Stark "dispersion function", can be written:

$$D_s(\nu) = \sum_M \beta_M(\nu), \quad (12)$$

where,

$$\beta_M(\nu) = (\alpha_M)_{\max} \frac{(\nu - \nu_M)(\Delta\nu)_M}{(\nu - \nu_M)^2 + (\Delta\nu)_M^2}. \quad (12a)$$

The quantity $\beta_M(\nu)$ is the dispersion component of ϵ_1 due to the M -th Stark component.

By replacing $\alpha(\nu)$ and $\beta(\nu)$ in Eq. (9) by $F_s(\nu)$ and $D_s(\nu)$, respectively, the power $P_{Ag}^{(s)}$ absorbed by the detector when a Stark field is applied becomes:

$$P_{Ag}^{(s)} = A \left\{ \left[\frac{1}{Q_L} + \lambda_0 F_s(\nu) \right]^2 + \left[\frac{\nu}{\nu_a} - \frac{\nu_a}{\nu} - \lambda_0 D_s(\nu) \right]^2 \right\}^{-1}. \quad (13)$$

For the determination of line intensity the important quantity is ΔP_{Ag} , the change of the absorbed power due to the Stark splitting of the line. From Eqs. (9) and (13) follows:

$$\Delta P_{Ag} = P_{Ag}^{(s)} - P_{Ag} = AN(\nu)/D(\nu), \quad (14)$$

where:

$$\begin{aligned} N(\nu) = & \lambda_0 \left\{ [\alpha(\nu) - F_s(\nu)] \cdot \left[\frac{2}{Q_L} + \lambda_0 \alpha(\nu) + \lambda_0 F_s(\nu) \right] - \right. \\ & \left. - [\beta(\nu) - D_s(\nu)] \cdot \left[2 \left(\frac{\nu}{\nu_a} - \frac{\nu_a}{\nu} \right) - \lambda_0 \beta(\nu) - \lambda_0 D_s(\nu) \right] \right\} \\ D(\nu) = & \left\{ \left[\frac{1}{Q_L} + \lambda_0 F_s(\nu) \right]^2 + \left[\frac{\nu}{\nu_a} - \frac{\nu_a}{\nu} - \lambda_0 D_s(\nu) \right]^2 \right\} \\ & \cdot \left\{ \left[\frac{1}{Q_L} + \lambda_0 \alpha(\nu) \right]^2 + \left[\frac{\nu}{\nu_a} - \frac{\nu_a}{\nu} - \lambda_0 \beta(\nu) \right]^2 \right\} \end{aligned}$$

The expression (14) relates ΔP_{Ag} , and hence the output signal of the spectrometer to the absorption coefficient $\alpha(\nu)$ of the gas. As one is interested in the relation between ΔP_{Ag} and α_{\max} it seems obvious to take $\nu = \nu_a = \nu_0$. However, the procedure usually followed when measuring line intensities is to adjust ν and ν_a so as to obtain a maximum output signal. The question now arises for which values of ν and ν_a is ΔP_{Ag} maximum, and how is $(\Delta P_{Ag})_{\max}$ related to $\Delta P_{Ag}(\nu = \nu_a = \nu_0)$ ($\equiv \Delta P_{Ag}(\nu_0)$)?

It is clear that ΔP_{Ag} will be maximum for ν and ν_a in the neighbourhood of ν_0 . Moreover, α_{\max} , and hence $F_s(\nu_0)$ and $D_s(\nu_0)$, are usually small compared to $(Q_L \lambda_0)^{-1}$. Assuming: $\nu = \nu_0$ and $\nu_a = \nu_0 + \delta \nu_a$, and expanding ΔP_{Ag} in a Taylor series in the vicinity of $\nu_a = \nu_0$, one obtains:

$$\frac{\Delta P_{Ag}(\nu_a = \nu_0 + \delta \nu_a) - \Delta P_{Ag}(\nu_a = \nu_0)}{\Delta P_{Ag}(\nu_a = \nu_0)} \simeq 2Q_L \frac{D_s(\nu_0)}{\alpha_{\max}} \left(\frac{\delta \nu_a}{\nu_0} \right) - 8Q_L^2 \left(\frac{\delta \nu_a}{\nu_0} \right)^2 + \dots$$

The higher order terms are much smaller and can be neglected. From this expansion follows:

$$(\Delta P_{Ag})_{\max} \simeq \Delta P_{Ag}(\nu_a = \nu_0) + \frac{1}{8} \left[\frac{D_s(\nu_0)}{\alpha_{\max}} \right]^2,$$

for:

$$\nu_a \simeq \nu_0 \left[1 + \frac{1}{8Q_L} \frac{D_s(\nu_0)}{\alpha_{\max}} \right].$$

For $D_s(\nu_0) < 0.2 \alpha_{\max}$ the difference between $(\Delta P_{Ag})_{\max}$ and $\Delta P_{Ag}(\nu_a = \nu_0)$ is less than 0.5 percent, and the difference between ν_0 and ν_a at which ΔP_{Ag} is maximum, is less than $1/(40 Q_L)$. For $Q_L = 5 \cdot 10^3$, and $\nu_0 = 20 \text{ GHz}$, the latter difference is less than 0.1 MHz. Thus, ΔP_{Ag} is not very sensitive to a slight detuning of the cavity from the resonance frequency of the gas. As $D_s(\nu_0) < 0.2 \alpha_{\max}$ is quite easily obtained, $\nu_a = \nu_0$ may be assumed at the maximum of ΔP_{Ag} .

An answer to the question, for which applied frequency ν , ΔP_{Ag} is maximum is not easily obtained. An approximate solution of the problem can analytically be obtained only for α_{\max} , $F_s(\nu)$, and $D_s(\nu)$ very small compared to $(Q_L \lambda_0)^{-1}$. In all other cases the simplest way to obtain the frequency at which ΔP_{Ag} is maximum is the numerical evaluation of ΔP_{Ag} for frequencies in the neighbourhood of ν_0 , using approximate values of α_{\max} , $F_s(\nu_0)$, and $D_s(\nu_0)$.

The question has been investigated numerically in Ref. 6, Sect. 3.3. for a number of special cases. The results can be summarized as follows:

(a) In the case of a symmetrical Stark splitting pattern $(\Delta P_{Ag})_{\max}$ is equal to $\Delta P_{Ag}(\nu_0)$ irrespective of the strength of the applied field.

(b) For asymmetrical Stark splitting pattern $(\Delta P_{Ag})_{\max}$ is generally different from $\Delta P_{Ag}(\nu_0)$, the difference being determined primarily by the separation $\delta \nu_{M^*}$ and the peak-intensity ratio R_{M^*} of the unsplit line and its nearest (indicated by subscript M^*) Stark component. When the splitting is reasonably strong ($\delta \nu_{M^*} \gtrsim 3 \cdot \Delta \nu$), $(\Delta P_{Ag})_{\max} - \Delta P_{Ag}(\nu_0)$ is less than one percent provided $R_{M^*} \leq 0.6$. However, the difference $(\Delta P_{Ag})_{\max} - \Delta P_{Ag}(\nu_0)$ increases rapidly with decreasing splitting ($\delta \nu_{M^*} < 3 \cdot \Delta \nu$). At the same time

there is a shift of the frequency at which ΔP_{Ag} is maximum. This shift can become a considerable fraction of $\Delta\nu$. As a consequence of these effects (shift-effects in the following) it is difficult to deduce α_{\max} from $(P_{Ag})_{\max}$ at weak splittings.

The modulation depth $m_g(\nu)$ of the transmitted power due to the periodical interruption of the gas absorption will now be defined as:

$$m_g(\nu) = \frac{\Delta P_{Ag}(\nu)_{\max}}{P_{Ag}^{(s)}(\nu) + P_{Ag}(\nu)}, \quad (15)$$

where, ν is the applied frequency for which ΔP_{Ag} is maximum.

From the preceding follows that ΔP_{Ag} is maximum for $\nu_a = \nu_0$, and with sufficiently strong fields also for $\nu = \nu_0$. Thus, by taking $\nu = \nu_a = \nu_0$, and by substituting Eqs. (9), (13), and (14) into Eq. (15), the expression for $m_g(\nu_0)$ becomes:

$$m_g(\nu_0) = \frac{\frac{2\lambda_0}{Q_L} [\alpha_{\max} - F_s(\nu_0)] + \lambda_0^2 [\alpha_{\max}^2 - F_s^2(\nu_0) - D_s^2(\nu_0)]}{\frac{2}{Q_L^2} + \frac{2\lambda_0}{Q_L} [\alpha_{\max} + F_s(\nu_0)] + \lambda_0^2 [\alpha_{\max}^2 + F_s^2(\nu_0) + D_s^2(\nu_0)]}. \quad (16)$$

This is the desired relation between m_g , Q_L , and α_{\max} , valid for moderately strong and strong fields. At the latter fields $F_s^2(\nu_0)$ and $D_s^2(\nu_0)$ are small compared to α_{\max}^2 , while $\lambda_0 F_s(\nu_0)$ is usually small compared to $1/Q_L$. Neglecting $F_s^2(\nu_0)$, $D_s^2(\nu_0)$, and the $F_s(\nu_0)$ term in the denominator of Eq. (16), the expression for $m_g(\nu_0)$ reads:

$$m_g(\nu_0) = \frac{\frac{2\lambda_0}{Q_L} [\alpha_{\max} - F_s(\nu_0)] + (\lambda_0 \alpha_{\max})^2}{\frac{2}{Q_L^2} + 2 \frac{\lambda_0}{Q_L} \alpha_{\max} + (\lambda_0 \alpha_{\max})^2}. \quad (17)$$

With the *AiM*-method $m_g(\nu_0)$ is measured directly. To obtain α_{\max} , Eq. (17) has to be solved for this quantity. The result is:

$$\alpha_{\max} = \frac{A}{\lambda_0 Q_L} (1 - 1/2A + 1/2A^2 - \dots), \quad (18)$$

$$A = \frac{m_g(\nu_0) + \lambda_0 Q_L F_s(\nu_0)}{1 - m_g(\nu_0)}.$$

Only for $m_g(\nu_0)$ values higher than about 0.15 the A^2 -term in Eq. (18) needs to be taken into account.

§ 4. *The Stark absorption function for the $J=1 \rightarrow 2$, $\Delta M = \pm 1$ transitions in OCS.* It has been shown in § 3 that the absorption intensity at the resonance frequency of the line is given by α_{\max} when the Stark field is zero, and by

$F_s(\nu_0)$ for Stark fields different from zero. Since at sufficiently strong fields (see § 3) $m_g(\nu_0)$ is determined by the change in the absorption intensity due to the Stark splitting the peak intensity $(\alpha_{\max})_{\text{meas}}$ measured with the Stark cavity spectrometer can be written as:

$$(\alpha_{\max})_{\text{meas}} = \alpha_{\max} - F_s(\nu_0),$$

(19)

or

$$(\alpha_{\max})_{\text{meas}} = \alpha_{\max}[1 - F_s(\nu_0)/\alpha_{\max}].$$

Equation (19) makes it clear that for accurate measurements $F_s(\nu_0)/\alpha_{\max}$ has either to be made negligibly small compared to unity or it has to be known and corrected for. In the following both possibilities will be discussed for the case of carbonyl sulphide in a TE_{0m1} Stark cavity absorption cell as used in the present measurements. Usually, in this cavity only transitions with $\Delta M = \pm 1$ are detected.

At sufficiently high pressures ($\gtrsim 0.02$ mm Hg) the half-width of microwave absorption lines is determined mainly by molecular collisions. In the absence of power saturation or of any strong Stark-field "inhomogeneity" it may be assumed that at these pressures the unsplit line and its components have the same half-width. Power saturation broadening is generally different for the unsplit line and for the various Stark-components. The Stark-field inhomogeneity caused either by a non-uniform spacing between the two Stark conductors or by an imperfect top of the modulating square-wave voltage results in a M -dependent broadening of the components.

By assuming: $(\Delta\nu)_M = \Delta\nu$ for all values of M , and by substituting Eqs. (11) and (11a) into Eq. (19) one obtains:

$$(\alpha_{\max})_{\text{meas}} = \alpha_{\max} \left(1 - \sum_M \frac{R_M}{1 + A_M^2} \right)$$

(20)

with:

$$R_M = \frac{(\alpha_M)_{\max}}{\alpha_{\max}}, \text{ and } A_M = \frac{\nu_0 - \nu_M}{\Delta\nu} \equiv \frac{\delta\nu_M}{\Delta\nu}.$$

Herein, A_M is the frequency displacement of the M -th Stark component from the unsplit line measured in units of $\Delta\nu$.

Carbonyl sulphide is a linear molecule and its ordinary Stark effect is of the second order. A general treatment of the Stark effect corresponding to $\Delta J = +1$, $\Delta M = \pm 1$ rotational transitions in linear molecules is given in Ref. 6, Sect. 2.2.2. From the formulae given in this reference it can be proved that for the $J = 1 \rightarrow 2$ transition of OCS at 24.3 GHz:

$$R_M = \frac{1}{20}(2 \pm M)(3 \pm M), \text{ and } \delta\nu_M = C_s \cdot E^2,$$

(21)

with:

$$C_s \simeq -5.0 \cdot 10^{-8} [63M^2 - 5(M \pm 1)^2 - 32] \text{ MHz}(V/\text{cm})^{-2}.$$

In these expressions, E is the strength of the applied field in volts/centimetre, M the magnetic quantum number of the lower state of the transition ($M = -1, 0, +1$); the (+) sign placed before M corresponds with the $\Delta M = +1$, the (−) sign with the $\Delta M = -1$ transitions.

In Fig. 2 is given the splitting pattern calculated using Eq. (21) for $E = 1\,000\text{ V/cm}$. This figure reveals that the line is hard to split for two reasons: the component nearest to the unsplit line is the strongest, and the $\delta\nu_M$ of this component is small ($\sim 0.55\text{ MHz}$) even for this relatively strong field.

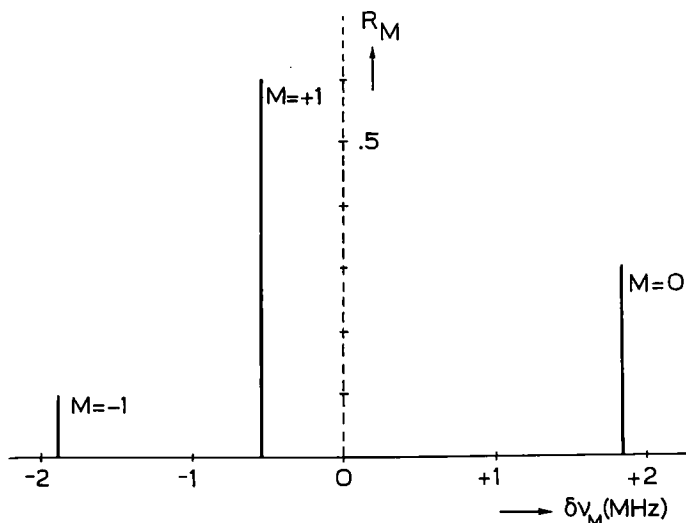


Fig. 2. Stark-splitting pattern of the $J = 1 \rightarrow 2$, $M \rightarrow M + 1$ rotational transition of OCS. The dashed line indicates the position of the unsplit line. The pattern of the $M \rightarrow M - 1$ transition is identical with the one of the $M \rightarrow M + 1$ transition but M has to be replaced by $-M$.

Measurements by Feeny *et al.*¹¹⁾ yield for the half-width of OCS at a temperature of 300°K :

$$\Delta\nu = 6.40\text{ MHz/mm Hg.} \quad (22)$$

By substituting this value of $\Delta\nu$, and the expression (21) for $\delta\nu_M$ and R_M into Eq. (20) it can be shown that $F_s(\nu_0)/\alpha_{\max}$ is less than 0.01 (corresponding to complete splitting) for:

$$E \gtrsim C_E \sqrt{P} \quad (23)$$

where $C_E \simeq 9.4 \cdot 10^3\text{ V/[cm(mm Hg)}^{\frac{1}{2}}]$, and P the pressure in mm Hg . Thus, for $P = 0.03\text{ mm Hg}$ a field of at least $1\,650\text{ V/cm}$ is required for a complete splitting.

The maximum field strength that can be obtained is generally limited by the maximum square wave voltage of the Stark generator and by the minimum permissible spacing between the two Stark conductors. When this

maximum field is not very strong (e.g. $\lesssim 1500$ V/cm) complete splitting cannot be obtained at pressures higher than, say, 0.03 mm Hg. There are, however, several objections against the use of very low pressures. Tuning difficulties, pressure drifts, frequency noise, power saturation of the gas, and Doppler broadening of the line become of rapidly increasing importance as the pressure is lowered. To minimize these difficulties it is profitable to work at higher pressures. As at these pressures the inequality (23) may not be satisfied the following methods can be used to obtain α_{\max} from $(\alpha_{\max})_{\text{meas}}$.

1st Method. With the aid of Eq. (21) the value of $F_s(\nu_0)/\alpha_{\max}$ can be calculated for any applied Stark field. The desired α_{\max} is thus obtained by measuring $(\alpha_{\max})_{\text{meas}}$ at a single (relatively high – see below) value of the applied field and by applying as a correction (Eq. (19)) the calculated value of $F_s(\nu_0)/\alpha_{\max}$.

The accuracy of this method can be increased in the following way. At a given pressure the line intensity is measured as a function of the applied field E . The obtained curve of $(\alpha_{\max})_{\text{meas}}$ versus E is then compared with a theoretical curve $C(E)$ (Eq. (19)):

$$C(E) = K[1 - F_s(\nu_0)/\alpha_{\max}], \quad (24)$$

calculated from Eqs. (20) and (21) for the pressure in question. The quantity $C(E)$ is simply $(\alpha_{\max})_{\text{meas}}/\alpha_{\max}$ multiplied by a constant K . The value of K which fits the calculated curve $C(E)$ to the experimental curve of $(\alpha_{\max})_{\text{meas}}$ versus E is the desired α_{\max} . A set of $C(E)/K$ curves is given in Fig. 3 for pressures of 0.02, 0.03, 0.04, and 0.05 mm Hg.

2nd Method. If the applied Stark field is strong enough to displace the component nearest to the unsplit line such that for this component $A_{M^*}^2 \gg 1$, Eq. (20) can be approximated in the following way (Eq. (21)):

$$(\alpha_{\max})_{\text{meas}} \simeq \alpha_{\max} \left(1 - \frac{R_{M^*}}{1 + A_{M^*}^2} \right) \simeq \alpha_{\max} (1 - C_\alpha E^{-4}). \quad (25)$$

Herein, M^* is the magnetic quantum number of the nearest Stark component and C_α a constant depending on R_{M^*} , $\delta\nu_{M^*}/E^2$, and $\Delta\nu$. Thus, as can be inferred from Eq. (25), the desired α_{\max} is obtained by extrapolating the measured curve of $(\alpha_{\max})_{\text{meas}}$ versus E^{-4} for $E^{-4} \rightarrow 0$, i.e. for an infinitely strong field.

The usefulness of the extrapolation procedure is limited mainly by the approximation $A_{M^*}^2 \gg 1$, which is justified only at relatively strong fields. In general, this method is quite useful for lines of which the splitting pattern is qualitatively known.

For the application of the first method R_M , $\delta\nu_M$, as well as $\Delta\nu$ must be known. This is, however, the case only for a limited number of lines. Moreover, it should be emphasized, that this method is applicable only if

the shift-effects (§ 3) can be neglected. At fields below a certain value the shift-effects become of increasing importance. At these fields the calculated $C(E)$ curve will not fit the experimental data.

§ 5. *Doppler broadening.* It is well known that at pressures higher than about 0.03 mm Hg the half-width of a microwave absorption line is proportional to the pressure and hence α_{\max} independent of the pressure (Ref.

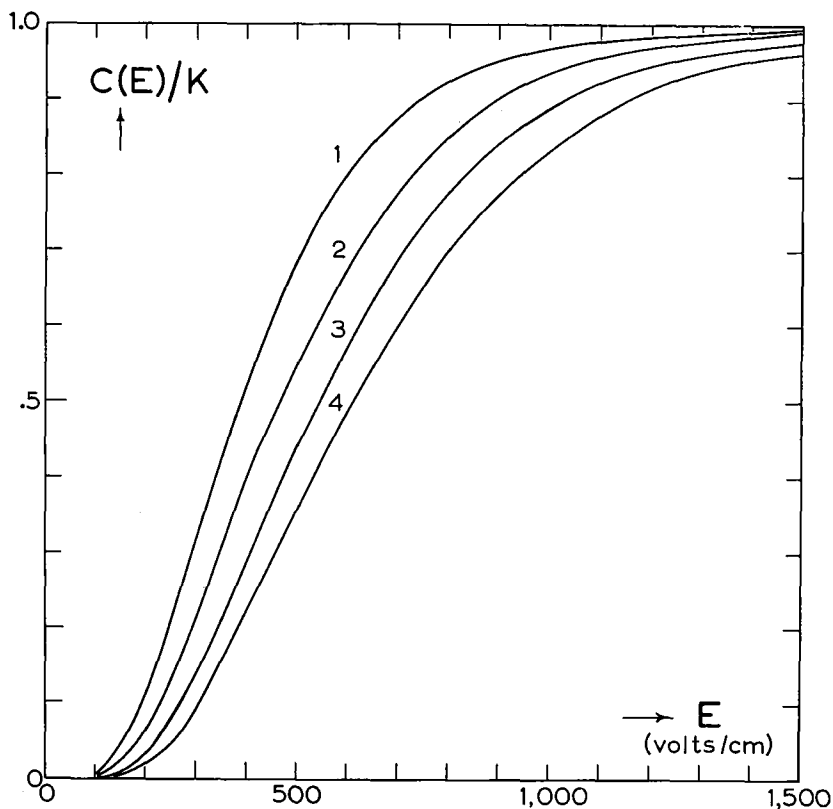


Fig. 3. The function $C(E)/K \approx 1 - F_s(\nu_0)/\alpha_{\max}$ for the $J = 1 \rightarrow 2$, $M \rightarrow M \pm 1$ rotational transition of OCS for pressures of 0.02 (curve 1), 0.03 (curve 2), 0.04 (curve 3), and 0.05 (curve 4) mm Hg.

6, p. 24). At pressures lower than this value, the broadening by the Doppler effect and the resulting decrease of α_{\max} have to be taken into account. The intensity of a line broadened only by the Doppler effect is proportional to $\exp[-(\nu - \nu_0)^2 \ln 2 / (\Delta\nu_{\text{Dopp}})^2]$, where $\Delta\nu_{\text{Dopp}}$ is the half-width of the line. The latter quantity is given by the expression (Ref. 10, p. 337):

$$\Delta\nu_{\text{Dopp}} = 3.581 \cdot 10^{-7} (\sqrt{T/M}) \cdot \nu, \quad (26)$$

in which, T is the absolute temperature, and M the molecular weight of the

gas. For OCS at room temperature ($T = 300^\circ\text{K}$) and at $\nu = 24.3\text{ GHz}$, $\Delta\nu_{\text{Dopp}}$ is about 19.5 kHz.

The shape of a line broadened both by molecular collisions and by the Doppler effect is described by the integral of Voigt ¹²). From this integral the peak intensity $\alpha^{(D)}_{\text{max}}$ in the presence of Doppler broadening is ¹³):

$$\alpha^{(D)}_{\text{max}} = C_D \left(\frac{a}{2} \right) \int_0^\infty \frac{e^{-y^2}}{(a/2)^2 + y^2} dy, \quad (27)$$

where:

$$a = 2 \ln 2 \cdot \frac{\Delta\nu_{\text{coll}}}{\Delta\nu_{\text{Dopp}}},$$

C_D is a constant independent of a , and $\Delta\nu_{\text{coll}}$ the half-width due to molecular collisions.

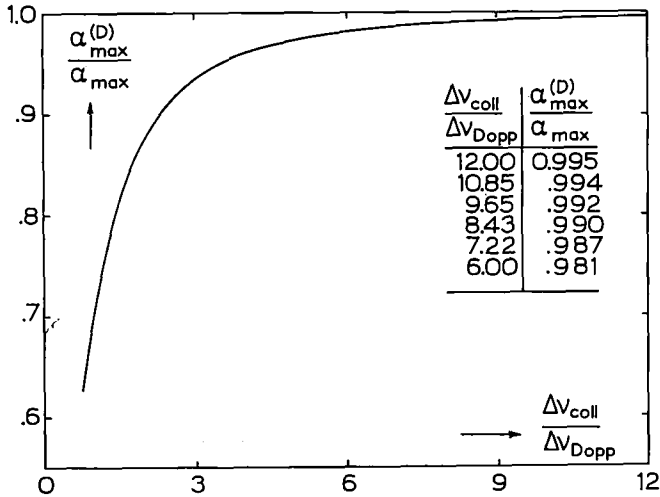


Fig. 4. Ratio $\alpha_{\text{max}}^{(D)}/\alpha_{\text{max}}$ as a function of $\Delta\nu_{\text{coll}}/\Delta\nu_{\text{Dopp}}$.

At high pressures, a is very large, and $\alpha^{(D)}_{\text{max}} = \alpha_{\text{max}}$. From Eq. (27) then follows:

$$\alpha_{\text{max}} = C_D \left(\frac{2}{a} \right) \int_0^\infty e^{-y^2} dy = C_D \frac{\sqrt{\pi}}{a},$$

and

$$\frac{\alpha^{(D)}_{\text{max}}}{\alpha_{\text{max}}} = \frac{a}{\sqrt{\pi}} \int_0^\infty \frac{e^{-(az/2)^2}}{1 + z^2} dz. \quad (28)$$

By substituting herein a known ¹⁴) solution of the integral one obtains for $\alpha^{(D)}_{\text{max}}/\alpha_{\text{max}}$:

$$\frac{\alpha^{(D)}_{\text{max}}}{\alpha_{\text{max}}} = \frac{\sqrt{\pi}}{2} a e^{(a/2)^2} [1 - \Phi(a/2)], \quad (29)$$

where $\Phi(a/2)$ is the error integral. In Fig. 4 is given a curve of $\alpha^{(D)}_{\text{max}}/\alpha_{\text{max}}$

calculated¹⁵) from Eq. (29) for $\Delta\nu_{\text{coll}}/\Delta\nu_{\text{Dopp}}$ values ranging from 1 to 12. It is shown in this figure that an appropriate correction ("Doppler correction" in the following) has to be applied to the measured intensities when $\Delta\nu_{\text{coll}}/\Delta\nu_{\text{Dopp}} \lesssim 10$.

PART II. EXPERIMENTAL APPARATUS

§ 6. *The spectrometer.* The Stark cavity spectrometer used in the present measurements was equipped with two detection schemes:

1. Superheterodyne detection (abbr. *SHD*) at the intermediate frequency of 30 MHz with Stark modulation at 400 Hz;
2. Straight-through detection (abbr. *STD*) with Stark modulation either at 10 kHz or at 400 Hz.

The latter scheme is relatively simple but because of its low sensitivity at power levels below 10^{-6} W it was suitable only for measurements on strong lines. For measurements on weak and/or easily saturable lines the *SHD*-scheme has been used throughout this research in spite of its complexity.

A simplified diagram of the *SHD*-spectrometer is shown in Fig. 5. But for a few changes the general outline of the *STD*-spectrometer was the same as of the *SHD*-spectrometer. The most important changes were: omission of the entire local-oscillator circuit, and substitution of the output amplifier chain starting with the *IF* amplifier by a set of amplifiers suited to the problem being investigated. For intensity measurements the crystal detector was followed by a low-noise narrow-band amplifier and a synchronous demodulator both tuned to the frequency of the modulating Stark field, in this case either 400 Hz or 10 kHz. The latter modulation frequency was also used when searching for absorption lines.

As the operation of both spectrometer types is well known only some features and components of the *SHD*-spectrometer are discussed below.

The attenuators A_1 , A_2 (Fig. 5) prevented frequency pulling of the signal-oscillator (abbr. *SO*-) and the local-oscillator (abbr. *LO*-) klystron, respectively. The primary object of the attenuators A_3 , A_4 , A_5 was the adjustment of the power entering the cavity. The attenuators A_4 and A_5 also reduced standing waves in the waveguide between the Stark cavity and the antimodulator. The uniline U_2 isolated the latter from the input circuit. A standing-wave meter was used for monitoring the *SO*-power and for calibration of the antimodulator. The *LO*-power applied to the mixer crystal M (Sylvania, 1N 26) through a directional coupler (DCP_3) was adjusted with the attenuator A_6 . A possible dependence of the Q_L -factor of the Stark cavity on microwave properties of its input and output lines¹ (Ref. 6, Sec. 3.1.1) was eliminated by using the uniline U_3 and the attenuator A_5 and by keeping the waveguides between U_3 , A_5 , and the cavity short.

The present spectrometer uses an IF of 30 MHz. The component of the mixer-crystal output at the intermediate frequency is first amplified by a low-noise amplifier tuned to 30 MHz and then demodulated by a synchronous

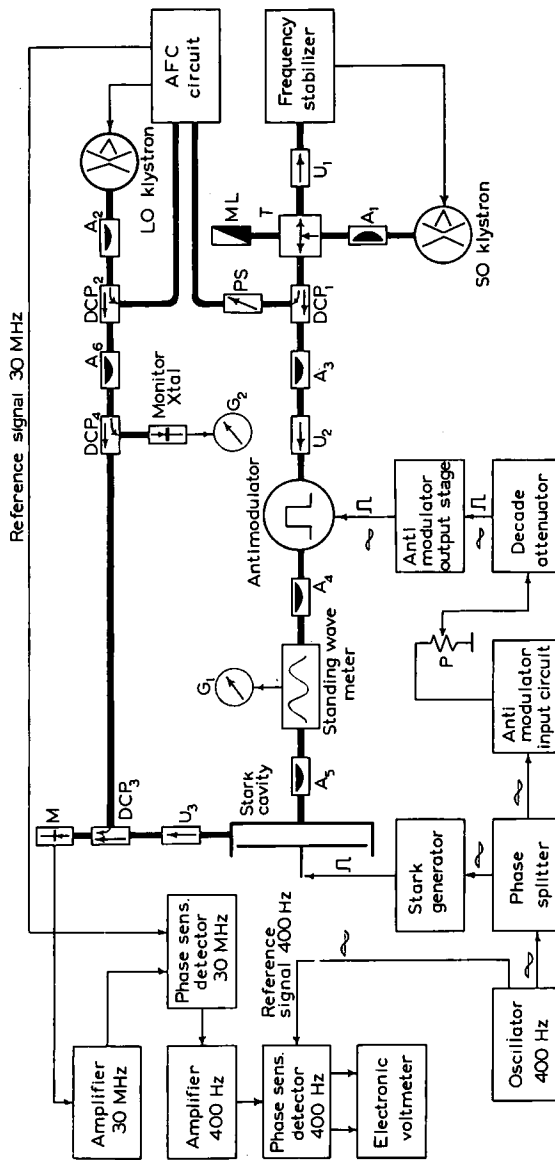


Fig. 5. Schematic diagram of the SHD-spectrometer; $A_1 - A_6$ = attenuators; $DCP_1 - DCP_4$ = directional couplers; G_1, G_2 = galvanometers; M = mixer crystal; ML = matched load; PS = phase shifter; P = potentiometer; T = magic T ; $U_1 - U_3$ = unilines.

detector. The latter is of the mixer type. The 30 MHz IF amplifier consists of a low-noise cascode input stage followed by a three-stage pentode amplifier of ordinary design. The reference voltage for the synchronous detector is taken from the IF amplifier of the automatic frequency control (abbr.

AFC)- circuit which effects a constant 30 MHz frequency difference between the *SO*- and the *LO*-klystron. Phase adjustment of the reference voltage is provided by a microwave phase shifter (*PS*) placed in the *SO*-power arm of the *AFC*-circuit.

The output of the 30 MHz synchronous detector is further amplified by a narrow-band amplifier tuned to 400 Hz, a modification of the circuit described by Sturtevant¹⁶⁾, and finally demodulated by a 400 Hz synchronous detector of the Schuster type¹⁷⁾. The output of the latter is applied to a pen recorder or to an electronic voltmeter through a low-pass filter. The most important components of the spectrometer: frequency stabilizer, *AFC*-circuit, Stark cavity, and antimodulators are discussed briefly in the following four sections.

§ 7. *Frequency stabilizer*. As shown in § 3 the *SO*-klystron has always to be tuned to the resonance frequency of the line. To avoid frequent retuning and uncontrolled variations of the measured intensities the *SO*-frequency must stay constant to within less than $0.1 \cdot \Delta\nu$ during the time required for a complete set of measurements on one particular line. For precision measurements on the OCS lines a stability of better than 20 kHz during at least 15 minutes was required.

This stability was obtained by locking the *SO*-klystron frequency to the resonance frequency of a reference cavity with the aid of an *IF* Pound stabilizer equipped with the "equal arm discriminator" of Zaffarano¹⁸⁾. Pound's original design was based on an *IF* of 30 MHz. The present stabilizer utilized an *IF* of only 455 kHz, which greatly simplified the electronic instrumentation without significant loss in stability.

§ 8. *The AFC-circuit*. The *AFC*-circuit was of conventional design. Owing to a large overall gain of this circuit the *LO*-frequency was quite stable if the *SO*-klystron was frequency stabilized.

However, with input powers to the Stark cavity below about $5 \cdot 10^{-7}$ W, variations of the measured m_g values of several percent were found when changing slightly the amplitude and/or phase of the *SO*-wave, also with the 30 MHz synchronous detector replaced by a (phase insensitive) diode. The main cause of the phenomenon was leakage of the *SO*-power through the microwave part of the *AFC*-circuit towards the output coupling of the Stark cavity. A fraction of this "leakage" power was coupled to the cavity, occasionally causing power saturation of the gas, the remainder was reflected to the mixer crystal. As the reflected power was also amplitude modulated by the absorption line the measured m_g value depended on the relative amplitudes and phases of the leakage *SO*-wave and the *SO*-wave passing the antimodulator.

In order to eliminate this source of error the *AFC*-circuit was disconnected

when working at very low power. The *LO*-klystron was then frequency stabilized by a 455 kHz Pound-Zaffarano stabilizer at a frequency differing by 30 MHz from the *SO*-frequency.

§ 9. *The Stark cavity.* Design considerations, construction, and performance of the Stark cavity are discussed in detail elsewhere ⁶⁾¹⁹⁾. For this paper it is sufficient to state that it was a cylindrical transmission cavity with a diameter of about 15 cm and a height adjustable from 0.4 to 1.7 cm. For absorption measurements the cavity could be used in any TE_{0m1} mode with m ranging from about 5 to about 12. The modulating Stark field was applied between the bottom and the plunger. A zero-biased square wave Stark voltage with an amplitude adjustable from 50 to 1 200 V peak-to-ground was supplied by a Stark generator utilizing in the final stage two gas discharge triodes connected in cascade and fired in succession by pulses obtained from a flip-flop circuit. The electric E vectors of the (static) Stark and microwave fields in the cavity are perpendicular to each other. As a consequence the observed Stark splitting pattern corresponds to the transitions $\Delta M = \pm 1$.

For intensity measurements the Q_L -factor of the Stark cavity and its frequency dependence have to be known with high accuracy (§ 2). In the present research the Q_L -factor was determined with the aid of the so-called modified dynamic method. With this method the response curve of the cavity is recorded with a number of superimposed frequency markers. From the known separations between the various markers the half-power bandwidth of the response curve and hence the Q_L -factor is determined in the ordinary way.

The method is relatively simple, quick, and very accurate. An accuracy of about one percent was currently achieved. Moreover, as the response curve is recorded without changing the microwave circuits coupled to the cavity the Q_L -factor obtained with this method is equal to the Q_L -factor effective during measurements of line intensities.

§ 10. *The antimodulators.* Two different types of antimodulators have been developed for use with the *AIM*-method: the Faraday modulator, and a vibrating attenuator.

The operation of the Faraday modulator is based on the microwave Faraday effect in a magnetized ferrite rod. The construction of this modulator ⁶⁾²⁰⁾, resembles closely that of the well known uniline. The component mostly differing from known designs is the circular waveguide section housing the ferrite rod. It was made of perspex, on the inside coated with an aluminium foil about 5μ thick. This design minimizes losses due to eddy currents at high modulation frequencies. Square wave modulation up to about 5 kHz was obtained in this way with a negligible distortion of the

waveform, and with some improvement, sine-wave modulation up to lower radio-frequencies seems to be possible. The magnetizing field for the ferrite rod was provided by a solenoid surrounding the perspex-guide section.

Using a Ferroxcube 4A rod of 10 cm length and 0.16 cm diameter, m_{AiM} , linearly depending on the current through the field solenoid, was obtained up to $m_{AiM} = 0.05$. The maximum obtainable m_{AiM} was about 0.15, but still higher values are possible with thicker rods. When the modulator was kept at a temperature constant to within 0.5°C the short- (Fig. 6) and the long-time reproducibility at a single frequency was about one percent. Unfortunately, m_{AiM} depended in an irregular way on microwave frequency.

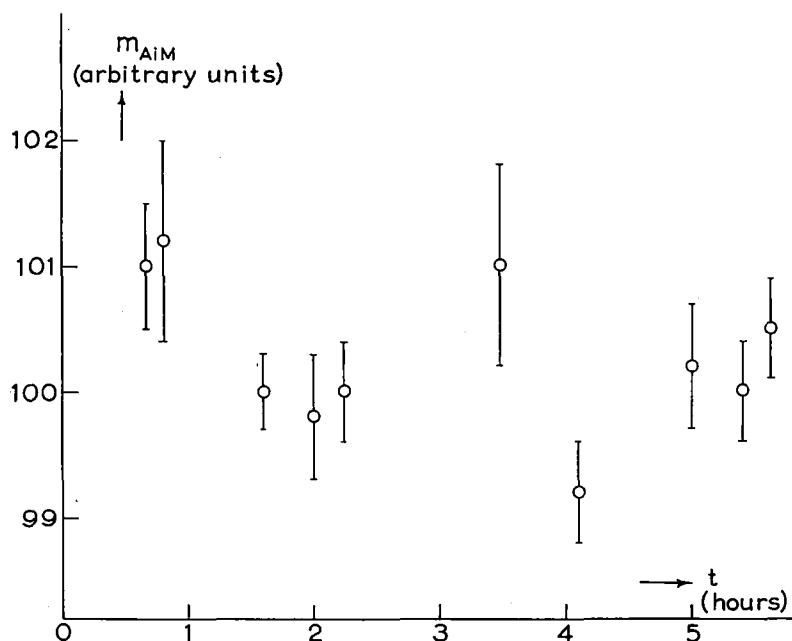


Fig. 6. Short-time reproducibility of m_{AiM} of the Faraday modulator.

Variations of m_{AiM} up to 10 percent have been observed over a frequency interval of only 100 MHz. The causes of these variations were presumably the dependence of the ferrite properties on microwave frequency, and (in spite of all efforts) reflections within the modulator.

The construction of the vibrating attenuator is shown in Fig. 7. To a coil suspended with the aid of two centring devices in the gap of a magnet is attached an attenuating strip, a sheet of mica coated with a carbon solution. This strip can be moved into a slotted section of a rectangular waveguide. A variable current sent through the coil results in a varying penetration of the strip into the guide and hence in a varying attenuation of the transmitted power. Under certain reasonable conditions the envelope of the

transmitted power is a faithful replica of the waveform of the current through the coil.

For a given constant AF voltage applied to the modulator the vertical movement of the coil decreases with increasing frequency. As a consequence the vibrating attenuator is suitable only for sine-wave modulation at frequencies lower than about 1 kHz, at least if $m_{AiM} \gtrsim 0.02$ is desired. In the present spectrometer sine-wave modulation at 400 Hz was used. At this frequency m_{AiM} values up to 0.08 were obtained with only a very slight deviation from proportionality between m_{AiM} and the voltage applied to the modulator coil.

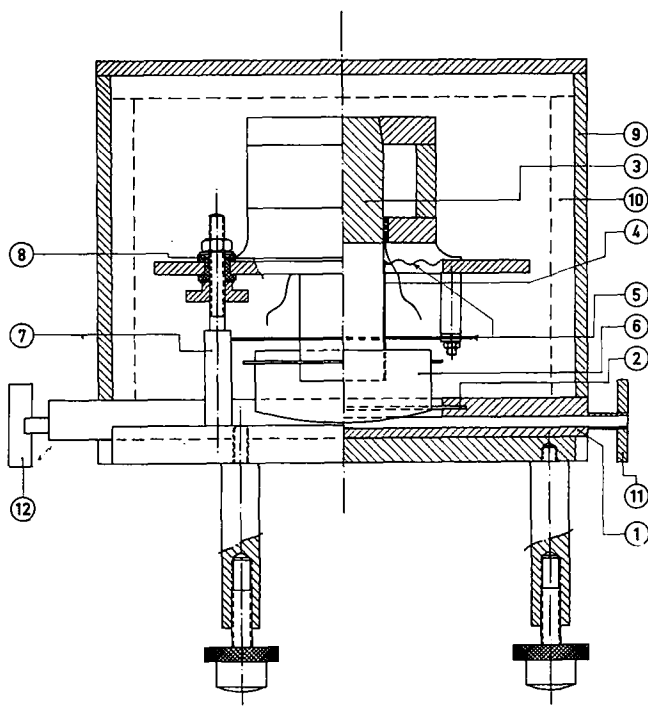


Fig. 7. Schematic drawing of the vibrating attenuator; (1) slotted section, (2) quarter-wave trap, (3) magnet-coil assembly, (4) perspex cylinder, (5) centring devices, (6) attenuating strip, (7) supports, (8) support insulators, (9) antimodulator housing, (10) sound-absorbing layer, (11, 12) coupling flanges.

The great advantages of the vibrating attenuator over the Faraday modulator are high stability of operation and independence of m_{AiM} on microwave frequency (Fig. 8), temperature, time, standing waves in the modulator waveguide, etc. The short-time and the long-time (over more than 50 days, Fig. 9) reproducibility was within about one percent.

The low-frequency circuit of the antimodulator was of conventional design. The modulating sine- or square-wave voltage from the input circuit

(Fig. 5) was applied to the output stage through a potentiometer P and a four-step high precision decade attenuator having a constant input impedance of $10\text{ k}\Omega$. The purpose of the potentiometer is explained below. In the case of the Faraday modulator the output stage was a cathode follower with the field solenoid in the cathode lead. For the vibrating attenuator this stage was a power tube operated in class A , matched to the low impedance ($\sim 7\Omega$) of the modulator coil with a step-down transformer.

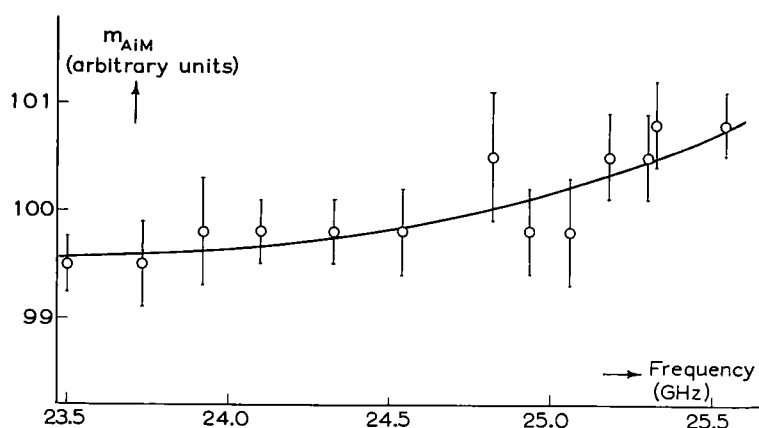


Fig. 8. Dependence of m_{AiM} of the vibrating attenuator on microwave frequency.

§ 11. *Calibration of the antimodulators.* The purpose of the calibration is to determine the relation between m_{AiM} and the voltage (or current) applied to the antimodulator.

The calibration method used in this investigation was based on the relation ⁴⁾⁶⁾:

$$m_{AiM} = \frac{C_A}{n} \left(\frac{i_\omega}{i_{DC}} \right), \quad (30)$$

$$C_A = \begin{cases} \pi/\sqrt{2} & \text{for square-wave modulation,} \\ 2\sqrt{2} & \text{for sine-wave modulation,} \end{cases}$$

between m_{AiM} , the rectified DC crystal current i_{DC} , the component i_ω of the crystal current at the modulation frequency ω , and the exponent n of the crystal response law (see Eq. (32)). The m_{AiM} of Eq. (30) is defined in the same way as m_g (Eq. (15)):

$$m_{AiM} = \frac{P_{\max} - P_{\min}}{P_{\max} + P_{\min}}. \quad (31)$$

Herein, P_{\max} is the maximum and P_{\min} the minimum instantaneous incident power on the crystal when the microwave signal is amplitude modulated.

Equation (30) is valid for a crystal detector assuming:

a) The relation between the rectified crystal current i and the incident wave voltage E is given by:

$$i(\cdot) E^n \quad (32)$$

with a constant value of the exponent n ;

b) i_{DC} , i_ω , and n are all determined at the same microwave power, with the same tuning of the microwave crystal circuit, and at the same non-reactive and frequency independent low-frequency loading of the crystal;

c) $m_{AiM} < 0.2$.

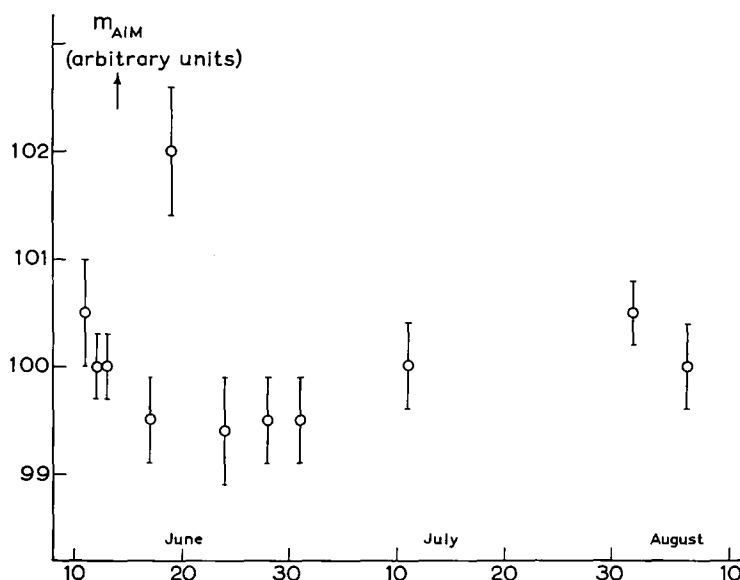


Fig. 9. Long-time reproducibility of m_{AiM} of the vibrating attenuator.

In the present research m_{AiM} did not exceed 0.1. The modulation frequency was usually 400 Hz. The low frequency loading of the crystal was pure resistive ($1\ 344\ \Omega$). The crystal (Sylvania, *1N26*) used for the calibration was connected to the microwave probe circuit of a high precision standing-wave meter. Both the probe circuit and the crystal were always tuned for the maximum i_{DC} . In order to satisfy also the assumption (a) the input power to the crystal was kept below $10^{-6}\ W$.

Determination of m_{AiM} thus required the measurement of three quantities: i_{DC} , i_ω , and n . The current i_{DC} ($\sim 10^{-7}\ A$) was measured with a sensitive galvanometer (Kipp, *A70HC*). The current i_ω was too small to be measured directly. Its value was obtained by making a well-known fraction f of a well-known (much greater) sine-wave voltage V_c at the modulation frequency, equal to the voltage V_ω built by i_ω across the crystal load resistor R_L .

Thus, i_ω is:

$$i_\omega = f \frac{V_c}{R_L}.$$

The voltage V_c was measured with a calibrated AC voltmeter (Philips, GM6015).

For the determination of n , use has been made of Eq. (32) and of the known power distribution along a short-circuited waveguide connected to a matched generator. It is well known (Ref. 8, p. 497) that, under certain conditions, the power $P(x)$ at a point x in such a waveguide is given by:

$$P(x) = P_0 \sin^2 2\pi x/\lambda_g, \quad (33)$$

where x is the distance to a point at which $P(x) = 0$, λ_g the guide wavelength, and P_0 is the power at $x = \lambda_g/4$. The power distribution $P(x)$ was investigated with the standing-wave meter mentioned previously. As the power absorbed from the waveguide by the probe is proportional to $P(x)$, the current $i_{DC}(x)$ through the crystal connected to the probe is:

$$i_{DC}(x) = (i_{DC})_{\max} \sin^n 2\pi x/\lambda_g. \quad (34)$$

With the aid of this expression the value of n can be obtained from the measured $i_{DC}(x)$ distribution.

A straightforward procedure has been followed for the calibration of the antimodulators. As the value n was found to be independent of time over a period of more than eight months, and also of microwave frequency (between 22 and 26 GHz), it was redetermined only from time to time. Thus the calibration was usually reduced to the measurement of i_{DC} and i_ω . For the measurement of the latter quantity the potentiometer P (Fig. 5) in the low-frequency circuit of the antimodulator was always adjusted such, that there existed a certain preassigned voltage across the coil of the vibrating attenuator, or a certain preassigned current through the field solenoid of the Faraday modulator when the decade attenuator was set at zero attenuation.

The estimated error in the value of m_{AtM} was about 1.8 percent, while the standard error of a set of measurements varied from 0.4 to 0.8 percent. The largest contributions to the RMS error come from the error in the value of n (~ 0.7 percent), the calibration error of galvanometer (~ 0.5 percent) and electronic AC voltmeter (~ 1 percent), and the reading error of the preassigned voltage or current (~ 0.7 percent).

PART III. RESULTS AND DISCUSSION

§ 12. *The experimental procedure.* Proper tuning of the spectrometer is one of the most essential conditions for good accuracy of the present method. Both the STD- and the SHD-spectrometer are quite easily tuned for

maximum output signal. In the case of the *STD*-spectrometer this tuning is identical with the tuning for the maximum modulation depth $(m_g)_{\max}$. However, this is generally not true in the case of the *SHD*-spectrometer if the *LO*-frequency is not properly set (Ref. 6, Sec. 5.3). Actually, for the evaluation of α_{\max} from Eq. (18), the spectrometer has to be tuned for $m_g(\nu_0)$. It has been shown in § 3 that $(m_g)_{\max} = m_g(\nu_0)$ only at sufficiently strong Stark fields.

For the above reasons the spectrometer was always tuned for $(m_g)_{\max}$ at the highest possible Stark field and at roughly the same pressure as the one used during the measurements. The tuning procedure was quite straightforward. The resonance frequency of the cavity, the *LO*- and *SO*-frequencies were adjusted in succession until a maximum m_g was obtained. At each setting of the three frequencies the output signal of the spectrometer was balanced to zero with the antimodulator. It is a special property of the *AIM*-method that a change in the output meter reading can then be caused only by a change of m_g .

Presence of power saturation was carefully controlled by checking power dependence of the measured intensities. Most of the measurements were performed with the *SHD*-spectrometer at an input power to the cavity varying from 10^{-7} to 10^{-9} W. No power saturation was observed at these power levels. For measurements on lines weaker than about $5 \times 10^{-7} \text{ cm}^{-1}$ the input power had to be increased slightly. This led to a weak (about one percent) power saturation of these lines at pressures below about 0.03 mm Hg. The measured intensities were corrected for this effect.

All measurements at pressures below 0.03 mm Hg were corrected for Doppler broadening with the aid of the graph in Fig. 4. The maximum correction applied was about two percent.

During the first (April–September 1957) series of measurements some difficulties were encountered from pressure drifts which, generally, tended to reduce the line intensities. These drifts were caused by small vacuum leaks, by release of foreign gases by metal and dielectric surfaces, and by adsorption of the gas on the latter surfaces. In order to eliminate these sources of errors the line intensity was measured as a function of time at a preassigned (usually the highest possible) Stark field. In this way a graph was constructed of line intensity versus time. Extrapolation of this graph to time zero (time of the gas admission) yielded the line intensity unaffected by pressure-drift effects. By improving the entire vacuum system of the spectrometer the pressure-drift effects were practically unimportant during the later series of measurements (September 1957–September 1958).

All measurements have been performed in the TE_{061} mode of the cavity. The pressure varied from 0.018 to 0.050 mm Hg, and the temperature from 23 to 24°C. At all pressures the line intensity was measured as a function of the applied Stark field. The field strength that could be obtained with

the maximum available square wave Stark voltage ($\sim 1\,200$ V, zero biased) was about $1\,700$ V/cm in the TE_{061} mode of the cavity at the frequency of 24.3 GHz. With this maximum field strength all OCS-lines could be split completely at pressures below about 0.027 mm Hg (Eq. (23)). At higher pressures the desired asymptotic value of $(\alpha_{\max})_{\text{meas}} (= \alpha_{\max}, \text{Eq. (19)})$ was obtained by the methods explained in § 4. The pressure could be measured with an accuracy of about two percent with a precision micromanometer.

The primary quantity which was determined with the AiM -method was setting of the decade attenuator at which the antimodulation cancelled the Stark modulation. The desired value of m_{AiM} was obtained from this setting with the aid of an appropriate calibration graph. In the case of the Faraday modulator (square wave AiM) m_g was equal to m_{AiM} . In the case of the vibrating attenuator (sine wave AiM) the antimodulation only cancels the signal sidebands at the fundamental frequency of the modulating square wave Stark field. Thus for the vibrating attenuator m_g is:

$$m_g = \frac{\pi}{4} m_{AiM}.$$

Finally, the absolute peak intensity was obtained from Eq. (18) by substituting therein the known value of λ_0 and the measured values of Q_L and $m_g(v_0)$. It should be noted that $F_s(v_0)$ in Eq. (18) has to be put equal to zero as it has already been eliminated by the methods of § 4. Generally, for relative measurements on closely spaced lines only the values of $m_g(v_0)$ for the two lines had to be known.

§ 13. *Results.* Absolute intensity measurements have been performed on seven lines of OCS, all arising from the $J=1 \rightarrow 2$ rotational transition. The most intense line of this series (the "main line" in the following) is assigned to the $^{16}\text{O}^{12}\text{C}^{32}\text{S}$ molecule, two other lines to the isotopic species $^{16}\text{O}^{13}\text{C}^{32}\text{S}$ and $^{16}\text{O}^{12}\text{C}^{34}\text{S}$, all three in the ground vibrational state. The remaining four lines arise from the $^{16}\text{O}^{12}\text{C}^{32}\text{S}$ molecule in four excited vibrational states: $(v_1v_2^{11}v_3) = (100), (01_1^10), (01_2^10), (02^00)$. In this designation of the vibrational states of a linear molecule (Ref. 10, p. 35) v_1 and v_3 are the quantum numbers of the symmetrical and antisymmetrical stretching vibration, respectively, and v_2 the quantum number of the degenerate bending vibration. The subscripts 1 and 2 of the states $v_2 = 1^1$ denote the lower and the higher component, respectively, of the so-called l -doublet (Ref. 10, p. 31). The frequencies of the seven lines are given in Table I.

Relative measurements have been performed on the first six lines listed in Table I. The line of $^{16}\text{O}^{12}\text{C}^{34}\text{S}$ is separated from other measured lines by more than 500 MHz. It was not possible to retune the spectrometer over this frequency interval before the line intensity was reduced by the pressure-drift effects by less than, say, three percent. For this reason measurements were not performed on this line.

TABLE I

| Measured peak intensities of the $J = 1 \rightarrow 2$ transition of OCS | | | | | | | |
|--|---|--|-----------------|-------------------------------------|-------------------------------|------------------------------|------------------------|
| Line No. | Species | Vibrational state ($\nu_1\nu_2^1\nu_3$) | Frequency (GHz) | α_{\max} (cm ⁻¹) | | Baird and Bird ⁴⁾ | |
| | | | | This paper | | | |
| | | | | Absolute | Relative | | |
| 1 | ¹⁶ O ¹² C ³² S | ground | 24.3259 | (5.13 ± 0.12)10 ⁻⁵ | 1.000 | (5.1 ± 0.7)10 ⁻⁵ | 4.4 × 10 ⁻⁶ |
| 2 | ¹⁶ O ¹³ C ³² S | ground | 24.2477 | (5.69 ± 0.13)10 ⁻⁷ | (1.10 ± 0.02)10 ⁻² | | 5.5 × 10 ⁻⁷ |
| 3 | ¹⁶ O ¹² C ³² S | (100) | 24.253 | (7.8 ± 0.2)10 ⁻⁷ | (1.51 ± 0.03)10 ⁻² | | 8.5 × 10 ⁻⁷ |
| 4 | ¹⁶ O ¹² C ³² S | (01 ₁ ¹ 0) | 24.3555 | (2.56 ± 0.06)10 ⁻⁶ | (4.93 ± 0.05)10 ⁻² | | |
| 5 | ¹⁶ O ¹² C ³² S | (01 ₂ ¹ 0) | 24.380 | (2.54 ± 0.06)10 ⁻⁶ | (4.93 ± 0.06)10 ⁻² | | |
| 6 | ¹⁶ O ¹² C ³² S | (0200) | 24.401 | (3.06 ± 0.08)10 ⁻⁷ | (5.90 ± 0.12)10 ⁻³ | | |
| 7 | ¹⁶ O ¹² C ³⁴ S | ground | 23.731 | (2.06 ± 0.05)10 ⁻⁶ | | | 2.3 × 10 ⁻⁶ |

In Fig. 10a is given the measured peak intensity of the main line at a number of applied Stark fields ranging from about 400 to about 1 6000 V/cm. In this figure is also given a curve of $C(E)$ calculated for a pressure of 0.020 mm Hg with the aid of Eq. (24). The value of the constant K was in this case chosen so as to make the experimental and theoretical values of the line intensity equal at a field of 1 000 V/cm. As can be seen, the experimental results are well fitted by the theoretical curve.

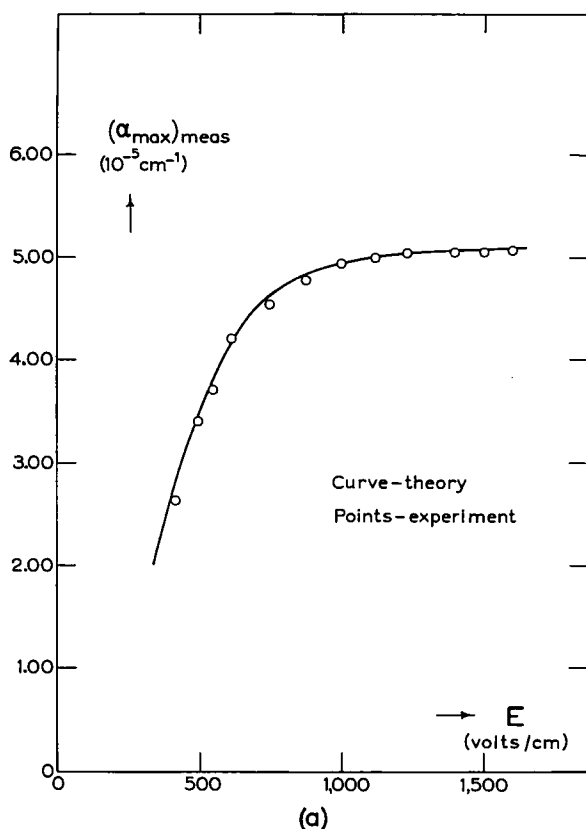


Fig. 10. (a) Measured and calculated peak intensity $(\alpha_{\max})_{\text{meas}}$ of the main line of OCS as a function of the applied Stark field E .

Application of the extrapolation procedure is illustrated in Fig. 10b, in which $(\alpha_{\max})_{\text{meas}}$ of the main line is plotted against E^{-4} . In this figure the experimental points obtained at fields higher than about 800 V/cm follow a straight line. Intersection of this line with the line $E^{-4} = 0$ yields the correct intensity of the line. At fields lower than 800 V/cm the measured values of α_{\max} are no more fitted by a straight line indicating that the approximations made in § 4 do not hold at these fields.

The results of the absolute and relative measurements are summarized in

Table I. The values of α_{\max} and of the intensity ratios given in this table are weighted mean values of four series of measurements performed in the period between April 1957 and September 1958. The total number of measurements on any line given in Table I is at least 30.

In Table I are also given the intensities obtained by Townes *et al.*²⁾, and by Baird and Bird⁴⁾. The intensity given by Townes *et al.* was obtained from absolute measurements, the intensities given by Baird and Bird from

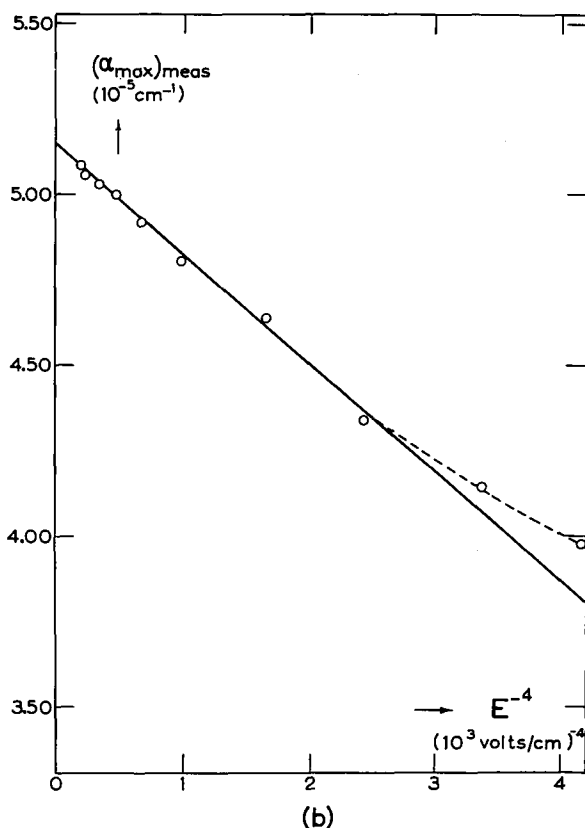


Fig. 10. (b) $(\alpha_{\max})_{\text{meas}}$ of the same line as a function of E^{-4} .

relative measurements assuming an intensity of $2.9 \times 10^{-7} \text{ cm}^{-1}$ for the $J = 1 \rightarrow 2$ line of $^{16}\text{O}^{12}\text{C}^{33}\text{S}$ in the ground vibrational state. This is a calculated intensity reported by Kisliuk and Townes²¹⁾. According to Baird and Bird the accuracy of their measurements was about 12 percent.

§ 14. *Discussion.* The estimated RMS error of the absolute intensities is about 2.5 percent for all lines listed in Table I. The major contributions to this error stem from the calibration error of the antimodulator (~ 1.8 percent), the error in Q_L (~ 1 percent), and the error in the asymptotic

value of $(\alpha_{\max})_{\text{meas}}$. The standard error in the mean value of a set of measurements on a single line varies from 0.2 to about 1 percent. The RMS error in relative measurements varies from about one to about two percent and is determined mainly by the error in the asymptotic value of $(\alpha_{\max})_{\text{meas}}$. The latter error also mainly limited the reproducibility of results. Both short-time (one day) and long-time (at least a month) reproducibility of absolute and relative intensities as indicated by the standard deviation was about two percent for the line $v_2 = 2^0$, and about one percent for all other lines. The intensity of the line $v_2 = 2^0$ was very sensitive to temperature changes.

In order to make a comparison between experiment and theory the peak intensities of the seven lines have been calculated (Ref. 6, Sect. 6.2.3) from a formula of Karplus and Schwinger⁹⁾ for $T = 296.5^\circ K$, the mean temperature at which most of the present measurements were performed. In these calculations the following values were assumed for the half-width $\Delta\nu$ ¹¹⁾, and for the electric dipole moment p (in Debye units)²²⁾:

$$\begin{aligned}\Delta\nu &= 6.40 \text{ MHz/mm Hg at } T = 300^\circ K (\Delta\nu(\cdot)T^{-1}), \\ p &= 0.700 \text{ for the } l\text{-doublet of } ^{16}\text{O}^{12}\text{C}^{32}\text{S}, \\ p &= 0.709 \text{ for all other lines.}\end{aligned}$$

The results, accurate to within about two percent are given in Table II, Column 4. In Column 5 of the same table are also given the intensities calculated by Kisliuk and Townes²¹⁾ assuming $T = 300^\circ K$, $\Delta\nu = 6 \text{ MHz/mm Hg}$, $p = 0.694$ for the l -doublet of $^{16}\text{O}^{12}\text{C}^{32}\text{S}$, and $p = 0.732$ and 0.722 for all other vibrational states of $^{16}\text{O}^{12}\text{C}^{32}\text{S}$ and $^{16}\text{O}^{13}\text{C}^{32}\text{S}$, respectively. At present these values are well known to be in error varying from 1 to 6 percent (see above). With the aid of the relation (Ref. 6, p. 22): $\alpha_{\max}(\cdot) p^2/(T^3 \Delta\nu)$ it is possible to correct the results of Kisliuk and Townes for the more recent values of p and $\Delta\nu$, and for $T = 296.5^\circ K$. For lines arising from transitions in excited vibrational states, a correction has also to be applied for the temperature dependent population of these states and for the change of the dipole moment matrix elements for transitions involving excited bending vibrational states. This change has apparently not been taken into account by Kisliuk and Townes. The corrected values are given in the last column of Table II. As can be seen from this table the corrected values of Kisliuk and Townes and the values of the present calculations are the same for the lines Nos 1 and 2, and differ only by about 2.5 percent for the lines Nos 3 and 7. In view of the good agreement for these four lines it is not clear why the values of Kisliuk and Townes are about 12 percent higher than the present ones for the l -doublet, and almost a factor of four higher for the line $v_2 = 2^0$.

Within the experimental error of about 2.5 percent, and the 2 percent error in the calculated intensities, the intensities of the lines Nos 1–4 and 7, as measured with the present method, are in good agreement with the

TABLE II

| Calculated peak intensities of the $J = 1 \rightarrow 2$ transition of OCS. | | | | | |
|---|---|--|-------------------------------------|-----------------------------------|--|
| Line No. | Species | Vibrational state ($v_1 v_2 l v_3$) | α_{\max} (cm ⁻¹) | | |
| | | | Dymanus ⁶⁾ | Kisliuk and Townes ²¹⁾ | Corrected values of Kisliuk and Townes |
| 1 | ¹⁶ O ¹² C ³² S | ground | 5.00×10^{-5} | 5.5×10^{-5} | 4.97×10^{-5} |
| 2 | ¹⁶ O ¹³ C ³² S | ground | 5.54×10^{-7} | 5.9×10^{-7} | 5.50×10^{-7} |
| 3 | ¹⁶ O ¹² C ³² S | (100) | 7.61×10^{-7} | 8.7×10^{-7} | 7.5×10^{-7} |
| 4 | ¹⁶ O ¹² C ³² S | (01 ₁ ¹ 0) | 2.83×10^{-6} | 4.4×10^{-6} | 3.16×10^{-6} |
| 5 | ¹⁶ O ¹² C ³² S | (01 ₂ ¹ 0) | 2.84×10^{-6} | 4.4×10^{-6} | 3.16×10^{-6} |
| 6 | ¹⁶ O ¹² C ³² S | (02 ⁰ 0) | 2.93×10^{-7} *) | 1.3×10^{-6} | 1.11×10^{-6} |
| 7 | ¹⁶ O ¹² C ³⁴ S | ground | 2.05×10^{-6} | 2.2×10^{-6} | 1.99×10^{-6} |

*) By assuming erroneously the (02⁰0) state of OCS as being doubly degenerate a value of 5.86×10^{-7} cm⁻¹ was previously obtained for this line ⁶⁾. The author is greatly indebted to Professor M. W. P. Strandberg of M.I.T. for pointing out this error.

intensities calculated for $T = 296.5^\circ K$. These results indicate that accurate absolute and relative intensity measurements are possible with the *AiM*-method.

However, agreement between the measured and calculated values breaks down for the *l*-doublet. According to the theory (Table II), the intensity of both components of the *l*-doublet should be about 1/17.6 of the intensity of the main line. From the present measurements follows, that within one percent the intensities of both components are indeed the same, but they are only about 1/20.5 of the main-line intensity. This discrepancy is far outside the error limits of the present method.

A possible origin of this discrepancy has been suggested by the author (Ref. 6, Sec. 6.2.4) and, in more detail by Strandberg ²³⁾. It is well known ²⁴⁾ that a linear molecule in an excited bending degenerate vibration is similar to a slightly asymmetric top which, in theoretical considerations, may be treated as a limiting form of a symmetrical top. The rotational energy associated with angular momentum along the symmetry axis of the molecule is just the vibrational energy of the bending vibration. As a consequence, when evaluating the sum over all rotational and vibrational energy states of the molecule one must not sum the energy associated with the bending vibration twice, once as apart of vibrational and once as a part of rotational energy. The intensities of the *l*-doublet line in Column 4,

Table II, have been calculated neglecting this effect of vibration-rotation interaction. A calculation which includes this effect is now in progress.

Acknowledgements. This investigation is part of the research program of the "Stichting voor Fundamenteel Onderzoek der Materie", and was made possible by financial support from the "Nederlandse Organisatie voor Zuiver Wetenschappelijk Onderzoek".

The author is greatly indebted to Professor E. F. M. van der Held for a helpful discussion on Doppler broadening, to Mr. A. Bouwknecht for his continuous assistance during the early stages of this investigation, and to Dr. L. H. Th. Rietjens and Mr. H. A. Dijkerman for reading the manuscript.

The pleasant helpfulness of Philips Research Laboratories, N.V. Philips' Gloeilampenfabrieken, Eindhoven, especially of Mr. H. G. Beljers, is gratefully acknowledged.

Received 6-5-59

REFERENCES

- 1) Beringer, R., Phys. Rev. **70** (1946) 53; Good, W. E., Phys. Rev. **70** (1946) 213; Becker, G. E. and Autler, S. H., Phys. Rev. **70** (1946) 300; Bleaney, B. and Penrose, R. P., Proc. Roy. Soc. **A189** (1947) 358; Strandberg, M. W. P., Meng, C. Y. and Ingersoll, J. G., Phys. Rev. **75** (1949) 1524.
- 2) Townes, C. H., Holden, A. N. and Merritt, F. R., Phys. Rev. **74** (1948) 1113.
- 3) Johnson, H. R. and Strandberg, M. W. P., J. Chem. Phys. **20** (1952) 687; Prokhorov, A. M. and Barchukov, A., J. Exp. Theor. Phys. U.S.S.R. **26** (1954) 761.
- 4) Baird, D. H. and Bird, G. R., Rev. Sci. Instr. **25** (1954) 319.
- 5) Verdier, P. H. and Wilson, E. B. Jr., J. Chem. Phys. **29** (1958) 340; Mattauch, R. D. and Strandberg, M. W. P., Rev. Sci. Instr. **29** (1958) 717.
- 6) Dymanus, A., Intensity measurements in the microwave spectroscopy of gases, Thesis, Utrecht (March 1958).
- 7) Gordy, W., Rev. Mod. Phys. **20** (1948) 668.
- 8) Montgomery, C. G., Technique of microwave measurements, MIT Radiation Laboratory Series, Vol. 11, McGraw-Hill Book Company, Inc., New York (1947).
- 9) Karplus, R. and Schwinger, J., Phys. Rev. **73** (1948) 1020.
- 10) Townes, C. H. and Schawlow, A. L., Microwave spectroscopy, McGraw-Hill Book Company, Inc., New York (1955).
- 11) Feeny, H., Lackner, H., Moser, P. and Smith, W. V., J. Chem. Phys. **22** (1954) 79.
- 12) Voigt, W., Phys. Z. **14** (1913) 377.
- 13) Van der Held, E. F. M., Z. Phys. **70** (1931) 508.
- 14) Gröbner, W. and Hofreiter, N., Integraltafel II, Springer-Verlag, Wien und Innsbruck (1950) p. 66.
- 15) Jahnke, E. and Emde, F., Funktionentafeln, Teubner, B. G., Leipzig und Berlin (1933) p. 97-98.
- 16) Sturtevant, J. M., Rev. Sci. Instr. **18** (1947) 124.
- 17) Schuster, N. A., Rev. Sci. Instr. **22** (1951) 254.
- 18) Zaffarano, F. P., M. S. Thesis (unpublished), MIT (June 1947).
- 19) Dymanus, A., Rev. Sci. Instr. **30** (1959) 191.
- 20) Dijkerman, H. A., Huiszoon, C. and Dymanus, A., submitted to Appl. Sci. Res.
- 21) Kisliuk, P. and Townes, C. H., J. Research Nat. Bur. Standards **44** (1950) 611.
- 22) Shulman, R. G. and Townes, C. H., Phys. Rev. **77** (1950) 500.
- 23) Strandberg, M. W. P., private communication.
- 24) Strandberg, M. W. P., Wentink, T. Jr., and Hill, A. G., Phys. Rev. **75** (1949) 827.